Biochimica et Biophysica Acta 1787 (2009) 75–85

Contents lists available at ScienceDirect

Biochimica et Biophysica Acta

journal homepage: www.elsevier.com/locate/bbabio

In *Yarrowia lipolytica* mitochondria, the alternative NADH dehydrogenase interacts specifically with the cytochrome complexes of the classic respiratory pathway

Sergio Guerrero-Castillo, Miriam Vázquez-Acevedo, Diego González-Halphen, Salvador Uribe-Carvajal *

Instituto de Fisiología Celular, Universidad Nacional Autónoma de México, Mexico City, Mexico

ARTICLE INFO

Article history:
Received 3 March 2008
Received in revised form 15 October 2008
Accepted 16 October 2008
Available online 6 November 2008

Keywords:
Alternative NADH dehydrogenase
Cytochrome complex
Supercomplex
Yarrowia lipolytica mitochondria

ABSTRACT

In *Yarrowia lipolytica*, mitochondria contain a branched respiratory chain constituted by the classic complexes I, II, III and IV, plus an alternative external NADH dehydrogenase (NDH2e) and an alternative oxidase (AOX). The alternative enzymes are peripheral, single-subunit oxido-reductases that do not pump protons. Thus, the oxidation of NADH via NDH2e-ubiquinone-AOX would not contribute to the proton-motive force. The futile oxidation of NADH may be prevented if either NDH2e or AOX bind to the classic complexes, channelling electrons. By oxymetry, it was observed that the electrons from complex I reached both cytochrome oxidase and AOX. In contrast, NDH2e-derived electrons were specifically channelled/directed to the cytochrome complexes. In addition, the presence of respiratory supercomplexes plus the interaction of NDH2e with these complexes was evaluated using blue native PAGE, clear native PAGE, in-gel activities, immunoblotting, mass spectrometry, and N-terminal sequencing. NDH2e (but not the redirected matrix NDH2i from a mutant strain, *Δnubm*) was detected in association with the cytochromic pathway; this interaction seems to be strong, as it was not disrupted by laurylmaltoside. The association of NDH2e to complex IV was also suggested when both enzymes coeluted from an ion exchange chromatography column. In *Y. lipolytica* mitochondria the cytochrome complexes probably associate into supercomplexes; those were assigned as follows: I–III_2, I–IV, I–III_2–IV_4, III_2–IV, III_2–IV_2, IV_2 and V_2. The molecular masses of all the complexes and putative supercomplexes detected in *Y. lipolytica* were estimated by comparison with the bovine mitochondrial complexes. To our knowledge, this is the first evidence of supercomplex formation in *Y. lipolytica* mitochondria and also, the first description of a specific association between an alternative NADH dehydrogenase and the classic cytochrome pathway.

1. Introduction

In mitochondria from mammalians, plants and many yeast species, four multi-subunit respiratory complexes participate in the transfer of electrons to oxygen, and thus are considered the classic components of the respiratory chain. These are: NADH:ubiquinone oxido-reductase (complex I), succinate:ubiquinone oxido-reductase (complex II), ubiquinol:cytochrome *c* oxido-reductase (complex III) and cytochrome *c* oxidase (complex IV). The respiratory chain generates a proton gradient used by the F_1F_0-ATP synthase (complex V) to synthesize ATP [1,2].

The mitochondrial respiratory complexes may associate into different supercomplexes. In mammalian systems, large supercomplexes containing I_1–III_2–IV_4 and III_2–IV_4 have been detected in BN-gels and seem to exist in a 2:1 stoichiometry [3]. In turn, these supercomplexes seem to associate into the larger "respiratory string" [4]. In plants, electron microscope images of supercomplexes I_1–III_2–IV_1 [5] and I_1–III_2 [6] have been reported. Using a similar approach, supercomplexes III_2–IV_2 [7] have been detected in *Saccharomyces cerevisiae*. In addition, a dimer of F_1-F_0-ATP synthase has been detected in beef heart [8], in *S. cerevisiae* and in *Polytomella* sp. [9–11]. Physiologically, supercomplex formation would be kinetically advantageous, as electrons would be directly channelled from one complex to the next [12]. In addition, highly reactive intermediates such as semiquinone would be sequestered by channelling, preventing their damaging effects [12]. Potentially, supercomplexes might also participate in regulation of oxidative phosphorylation [13].

In addition to the four classic respiratory complexes, plants, protozoa and fungi contain other mitochondrial redox enzymes that provide alternative pathways for electron flux [14]. The type II NAD(P)H dehydrogenases (NDH2) are peripheral proteins located on either the inner (NDH2i) or the outer (NDH2e) surface of the inner mitochondrial membrane (IMM). Alternative oxidases (AOX) are bound to the matrix-side of the IMM [15]. These alternative components do not pump protons; instead, they seem to participate in energy-dissipation, in heat-production and/or in prevention of ROS-generation [16,17]. In *S. cerevisiae* mitochondria, the association

* Corresponding author. Fax: 5255 5622 5630.
E-mail address: suribe@ifc.unam.mx (S. Uribe-Carvajal).

0005-2728/$ – see front matter © 2008 Elsevier B.V. All rights reserved.
doi:10.1016/j.bbabio.2008.10.008

of each of succinate dehydrogenase, NDH2i or NDH2e to the cytochrome chain was suggested from electron channelling data [18].

The mitochondrial respiratory chain of *Yarrowia lipolytica* contains one external NADH dehydrogenase (NDH2e) [19] plus two isoforms of AOX. In *Candida albicans*, which contains a similar respiratory chain, only one AOX is constitutively expressed [20]. Thus, by analogy it has been proposed that in *Y. lipolytica* one of the AOX is induced in the stationary phase [21]. NDH2e is a 60 kDa, single-subunit enzyme containing a non-covalently bound flavine-adenine-dinucleotide. NDH2e transfers electrons from external NADH to ubiquinone and is insensitive to the complex-I inhibitor rotenone, but sensitive to flavone or platanetin [22,23]. Aiming to analyse complex-I structure and function, mutants with impaired complex-I have been created (e.g. *Y. lipolytica Δnubm*). In these mutants, NDH2e was successfully redirected to the IMM matrix side (hereby called NDH2i) to rescue the deficiency in complex I [24].

AOX transfers electrons from ubiquinol to oxygen, bypassing complexes III and IV. At variance with complex IV, AOX does not pump protons and is insensitive to cyanide [25]. AOX is inhibited by hydroxamic acids or by alkyl-gallates [17]. Electron transfer from NADH to oxygen via NDH2e, ubiquinone and AOX, would not contribute to the proton gradient. Such an alternate pathway seems highly disadvantageous from an energetic point of view, and if functional, it should be subject to strict control. The flow of electrons following the path NDH2e-quinone-AOX would perhaps be desirable when the reducing power is in excess, a condition present at the stationary growth phase [16]. The resulting uncoupling would control the $NADH/NAD^+$ cytoplasmic ratio preventing ROS production [17]. In contrast, in the exponential growth phase the presence of this electron sink would probably be deleterious. Thus, we propose that at least during the exponential phase, the flux of electrons between the alternative enzymes (NDH2e and AOX) has to be prevented. This prevention would be achieved either through a possible interaction of AOX with complex I [26,27] and/or through an interaction of NDH2e with the cytochrome pathway.

In a study comparing 21 yeast species, Veiga et al. [26] observed that AOX and complex I always coexist, with the sole exception of *Pichia annomala*. In contrast, yeasts in which complex I is absent, also lack AOX [22,26]. This coexistence has led to suggest that complex I and AOX interact physically, channelling ubiquinone intermediaries [27]. Once associated with complex I, AOX would be indirectly implicated in energy conservation [26]. In this regard, in the filamentous fungus *Podospora anserina*, it was proposed that supercomplexes (I_2 and I_2–III_2) donate their electrons to AOX [27]. However, although it has been suggested [27], the physical interaction of AOX with these respiratory complexes has not been demonstrated [27,28].

In freshly isolated mitochondria from *Y. lipolytica* cells growing in the exponential phase, oxygen consumption data suggested that NDH2e channels electrons to the cytochrome complexes. In digitonin-solubilised mitochondria both the presence of cytochrome supercomplexes and the association of NDH2e to these complexes were detected. By contrast, AOX did not seem to associate to other components of the respiratory chain.

2. Materials and methods

2.1. Materials

Mannitol, sucrose, dextrose, pyruvate, malate, antimycin A, polyacrylamide, rotenone and SHAM were from Sigma Chem. Co. (St Louis, Mo, USA). Coomassie blue G was from Serva (Heidelberg, Germany). Polyclonal antibodies against *Y. lipolytica* NDH2e (anti-*Yl*NDH2e) were a kind gift from Dr. Stefan Kerscher, Zentrum der Biologischen Chemie, Frankfurt University, (Germany) and polyclonal antibodies directed against NDH2 of *Agrobacterium tumefaciens* (anti-*At*NDH) were a kind gift from Dr. Gilles Peltier, Commissariat à l'Énergie Atomique (France).

2.2. Strains, culture and isolation of yeast mitochondria

Y. lipolytica E150 (*MatB his1-1 ura3-302 leu2-270 xpr2-322*) and a complex I-subunit deletion strain, *Δnubm* [23] were a kind gift from Prof. Ulrich Brandt, ZBC, Frankfurt University (Germany). Cells were grown in YD (Yeast extract 1%, glucose 2%, [29]) at 160 rpm, 30 °C for 15 h and were harvested at the logarithmic growth phase. Cells were washed and resuspended in 5 mM MES, 0.6 M mannitol, 0.1% BSA (pH 6.8 adjusted with triethanolamine) and disrupted using a Bead Beater cell homogenizer (Biospec Products, OK, USA) with 0.45 mm glass beads (3×20 s pulses separated by 40 s resting periods). To isolate mitochondria, the homogenate was differentially centrifuged as described in [30] and protein concentration was determined by biuret [31].

2.3. Bovine heart mitochondria

Beef heart mitochondria obtained as in [32], were a kind gift from Dr. Marietta Tuena (IFC, UNAM). Considering that the molecular masses (MWs) for the beef heart mitochondrial oxidative phosphorylation complexes are well known [33], these were used as standards for BN-PAGE.

2.4. Oxygen uptake measurements

The rate of oxygen consumption was measured using a YSI model 5300 oxygraph with a Clark type electrode in a 1.5 ml water-jacketed chamber at 30 °C [34]. The oxygraph was interfaced to a PC with a voltmeter (Steren, MUL-600, Mexico). Phosphorylating and uncoupled states were induced by 1 mM ADP or 0.5 μM CCCP, respectively. The reaction mixture contained 0.6 M mannitol, 5 mM MES (pH 6.8), 20 mM KCl, 4 mM phosphate, 1 mM $MgCl_2$ and the indicated respiratory substrate: 1 mM NADH or 10 mM pyruvate/malate. Mitochondria were added to a final concentration of 0.5 (only when using NADH) or 1.0 mg protein/mL. Where indicated, 100 μM KCN or 50 μM propyl-gallate (PG) was added.

2.5. Blue native (BN) and clear native (CN) electrophoresis

BN- and CN-PAGE were performed as described in the literature, except for slight modifications [35,36]. Briefly, mitochondria were washed in 250 mM sorbitol, 50 mM Bis–Tris (pH 7.0), and centrifuged at 14,500 rpm for 10 min at 4°C. The pellet was resuspended in sample buffer [750 mM aminocaproic acid, 50 mM Bis–Tris (pH 7.0)] and solubilised with 2.0 g n-dodecyl-β-D-maltoside (laurylmaltoside, LM)/g protein, or 4.0 g digitonin (Dig)/g protein at 4 °C for 1.5 h and centrifuged at 30,000 rpm at 4 °C for 30 min. The supernatants (1 mg protein) were loaded on 4–12% polyacrylamide gradient gels. The stacking gel contained 4% (w/v) polyacrylamide. For CN-PAGE, digitonin (0.025%) was added to the gel preparation as described in [37]. When high resolution clear native electrophoresis was performed, 0.01% LM plus 0.05% deoxycholate were added to the cathode buffer as described in [38]. In order to perform 2D-SDS-Tricine-PAGE, complete lanes from either the BN- or CN-gels were loaded on 14% polyacrylamide gels to resolve the subunits that constitute each complex [39]. In order to enhance resolution, an outer longitudinal slice of the 1D-gel was cut on each side and only the 80% central section of the band was used. Apparent molecular masses were estimated from Benchmark protein standards (Invitrogen, CA, USA).

2.6. In-gel enzymatic activities

In-gel NADH/NBT oxido-reductase activity was determined by incubating the native gels in a mixture containing 10 mM Tris

(pH 7.0), 0.5 mg nitro blue tetrazolium bromide (NBT)/ml, 1 mM NADH [40,41]. When it was desired to simultaneously detect complex III and complex IV, in-gel cytochrome peroxidase activity was determined using tetramethyl benzidine as described in [42]. In-gel cytochrome *c* oxidase activity was determined using diaminobenzidine as described in [38]. In-gel ATPase was measured as in [37].

2.7. Ion exchange chromatography

Mitochondria were solubilised in 1 mM Mg-SO_4, 1 mM PMSF, 50 mM Tris, pH 8.0, plus 50 μg TLCK mL^{-1} added with 2 g LM(g prot)$^{-1}$. The solubilisate was centrifuged at 30,000 rpm for 30 min and layered on top of a previously equilibrated DEAE-Sepharose column [43]. Once loaded, the column was washed with 3 volumes of 1 mM $MgSO_4$, 50 mM Tris, pH 8.0 and proteins were eluted with a 0–400 mM NaCl gradient in the same buffer. Fractions (2.5 ml) were collected and the protein concentration of each fraction was determined spectrophotometrically at 280 nm.

2.8. Enzymatic activities in chromatography eluates

Each chromatography fraction was collected in a well within an Elisa multi-well plate and it was read in a BioRad 550 microplate reader equipped with different filters as specified below. Assayed activities were a) NADH dehydrogenase activity, following the reduction of nitro blue tetrazolium bromide (NBT) at 570 nm. The reaction mixture was 10 mM Tris, pH 7.0, 1 mM NADH, 0.5 mg mL^{-1} NBT; b) Cytochrome-*c* oxidase activity was measured in 50 mM phosphate buffer (sodium) pH 7.4, 2.5 mg mL^{-1} cytochrome *c*, 1 mg mL^{-1} diaminobenzidine and reduction was followed at 490 nm; c) ATPase activity was determined at 415 nm in 10 mM Tris–270 mM glycine, pH 8.0, 14 mM $MgSO_4$, 8 mM ATP (sodium salt); 0.2% Pb $(NO_3)_2$.

2.9. Immunoassays

From CN-, BN- or SDS-Tricine-PAGE, proteins were electrotransferred onto a nitrocellulose membrane (BioRad, Hercules, CA, USA) for immunodetection. Membranes were washed, blocked, and incubated with anti-*Yl*NDH2e [44] (1:1000 for 1 h) or with anti-*At*NDH [45] (1:1000 for 1 h), using an alkaline phosphatase-conjugated anti-rabbit IgG (1:3000 for 2 h) as secondary antibody. In order to further identify the different *Y. lipolytica* mitochondrial complexes, polyclonal antibodies against the iron–sulfur protein from bovine complex III [46], and against the beta subunit from the F_1F_o-ATP synthase from *Polytomella* sp. were used. Also, a monoclonal antibody against subunit III of cytochrome *c* oxidase (COX III) from *S. cerevisiae* (Mitoscience, Eugene, Ore, USA) was used. Ion exchange chromatography fractions were also subjected to SDS-Tricine-PAGE and immunoblotted with antibodies against either *Yl*NDH2e or COXIII.

2.10. Mass spectrometry and N-terminal sequencing

From the CN- or BN-gels, the indicated bands were excised from the gel and sent for protein sequence identification by LC-MS/MS to the Yale Cancer Center Mass Spectrometry Resource and W.M. Keck Foundation Biotechnology Resource Laboratory (New Haven, CT, USA). After tryptic digestion, samples were analysed in a tandem mass spectrometer. The automated Mascot algorithm was used to search all LC-MS/MS results against the NCBI database. Alternatively, N-terminal sequencing of some proteins was carried out by Dr. J. d'Alayer on an Applied Biosystems Sequencer at the Laboratoire de Microséquençage des Protéines, Institut Pasteur, Paris (France) [47].

2.11. Iso-electric point estimate of NDH2

The sequence of NDH2 was subjected to analysis using an open access program, "compute pI/MW" available at "Expasy Tools". This program predicted an isoelectric point of 8.45 for the native NDH2e at of 6.0 for the redirected, 101 residues shorter, NDH2i [23].

3. Results

3.1. Complex I-derived electrons access both cytochrome oxidase and AOX, while NDH2e-derived electrons are channelled to the cytochrome pathway

In order to determine the fate of the electrons that feed the respiratory chain from different sources, the inhibition of O_2 consumption by KCN, propyl-gallate (PG), or both, was evaluated in mitochondria from *Y. lipolytica* (*Yl*-mitochondria). Octyl-gallate and SHAM exhibited the same effects as PG (results not shown). The KCN- or PG-mediated inhibition was measured both in the uncoupled and in the phosphorylating states. Added NADH is oxidized directly by the external NADH dehydrogenase (NDH2e) while the pyruvate/malate mixture produces NADH in the matrix, which is then oxidized by complex I. The electrons from either NDH2e or Complex I reduce quinone to quinol; then quinol is reoxidized either by AOX or by complex III [2].

In the presence of pyruvate/malate, KCN inhibited the rate of O_2 uptake by 80% (Fig. 1A trace a), while the PG-mediated inhibition was 20% (Fig. 1A trace b). Neither KCN nor PG inhibited O_2 consumption completely, suggesting that the complex I-derived electrons could reach both the classic cytochrome pathway and AOX (Fig. 1A). The simultaneous addition of KCN and PG did result in complete inhibition (result not shown). In contrast, the NADH-supported respiration was fully sensitive to KCN (Fig. 1A, trace c), while no PG-mediated inhibition was detected (Fig. 1A, trace d). These results suggested that in *Yl*-mitochondria, NDH2e channels its electrons directly to the cytochrome pathway, i.e. the electrons from NDH2e do not reach AOX.

From the experiments above, the possibility arises that NDH2e is physically associated to the components of the classic cytochrome pathway. This was further explored in phosphorylating *Yl*-mitochondria. In the presence of pyruvate/malate, the partial sensitivity of ADP-induced respiration to KCN was still detected, and inhibition became complete only after adding PG (Fig. 1A, trace e). In contrast, when NADH was the respiratory substrate, inhibition by KCN was complete, although oxygen consumption was partially restored by pyruvate/malate; the restored uptake of oxygen was fully sensitive to PG (Fig. 1A, trace f). The complete inhibition of NADH-supported oxygen consumption by KCN indicates that in *Yl*-mitochondria the NDH2e-derived electrons are channelled to the classic cytochrome pathway via a putative localized quinone pool [18].

In the presence of different concentrations of KCN, the inhibition pattern of the respiratory chain was different depending on whether the substrate was pyruvate/malate or NADH. This is illustrated in a Dixon plot where it was observed that in the presence of NADH, KCN exhibited an apparent inhibition constant (Ki)=10 μM, plus a high linear correlation indicative of a simple inhibition system (Fig. 1B). In contrast, in the presence of pyruvate/malate, the Ki could not be calculated due to the non-linear behaviour observed, which nonetheless indicated that in this case the KCN-mediated inhibition of oxygen uptake was partial. These results again point to the existence of a KCN-resistant pathway in *Yl*-mitochondria detectable only in the presence of pyruvate/malate, most likely, the KCN-resistant AOX. Since KCN behaved as a noncompetitive inhibitor (Fig 1B), it was not necessary to vary the substrate concentration to obtain the Ki [48].

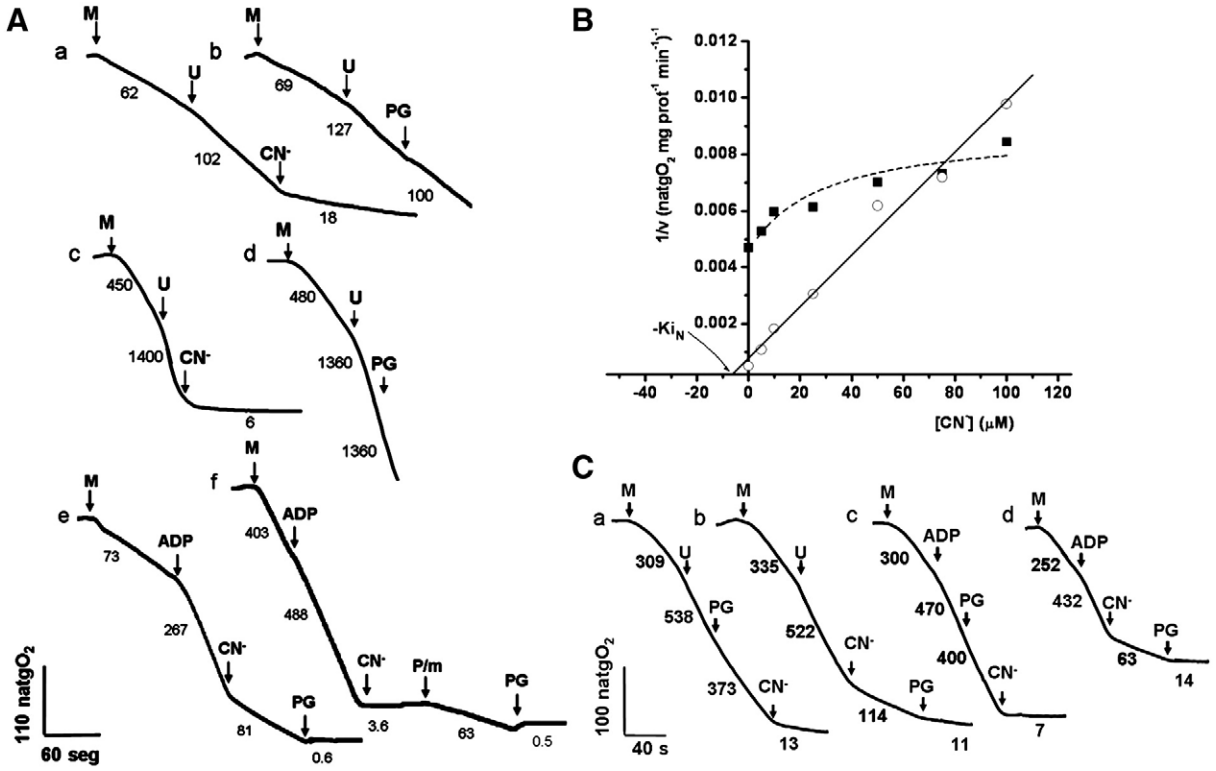

Fig. 1. Substrate dependence of the effect of KCN and propyl-gallate on the rate of oxygen consumption by mitochondria isolated from *Y. lipolytica*. Experimental conditions: 0.6 M mannitol, 5 mM MES (pH 6.8), 20 mM KCl, 1 mM $MgCl_2$, 4 mM phosphate–Tris (pH 6.8), 10 mM pyruvate/malate–Tris (pH 6.8) (traces a, b and e), or 1 mM NADH (traces c, d and f). Where indicated 0.5 μM CCCP (U), 1 mM ADP, 100 μM KCN (CN^-), or 50 μM propyl-gallate (PG) were added. Numbers indicate the rate of oxygen consumption in natg O_2 (mg $protein^{-1}$ min^{-1}). Representative experiments $n=5$. (A) Wild type mitochondria (M) at a concentration of 1 or 0.5 mg protein ml^{-1} (for pyr/mal or NADH, respectively). (B) Dixon plot of the oxygen consumption rates (in uncoupled state) in the presence of increasing KCN concentrations using 1 mM NADH (○) or 10 mM pyruvate/malate (■). (C) mitochondria isolated from the *Δnubm* mutant strain of *Y. lipolytica* used at a concentration of 1 mg protein ml^{-1}. Pyruvate/malate was used to feed the redirected alternative dehydrogenase (NDH2i). Traces a and b, effects on the uncoupled state; c and d, effects on state 3.

3.2. When NDH2 is redirected to the matrix side of the inner membrane, it reduces both cytochrome oxidase and AOX

A *Y. lipolytica* mutant strain (*Δnubm*) was created in the laboratory of Dr. U. Brandt by adding a mitochondrial presequence to NDH2e and thus redirecting the protein to the matrix face of the IMM (NDH2i) [23]. The expression of NDH2i in the *Δnubm* mutant rescued the lethality of the inactivation of complex I, demonstrating that NDH2i can oxidize the NADH in the mitochondrial matrix [23]. In *Δnubm*, we explored whether the redirected NDH2i still channelled electrons to the cytochrome pathway, observing that pyruvate/malate could still feed the respiratory chain; i.e. matrix-produced NADH was oxidized by NDH2i both in the uncoupled state and in state 3 (Fig. 1C). Nevertheless, in *Δnubm* mitochondria the addition of KCN (Fig. 1C, traces a and c) or PG (Fig. 1C, traces b and d) resulted in partial inhibition of oxygen consumption. Also, the KCN- and PG-mediated inhibition was additive (Fig. 1C). Thus, although NDH2i was fully functional, the electron channelling previously observed for NDH2e was lost, suggesting that the putative interaction between NDH2e and the cytochrome complexes involves specific protein domains located at the intermembrane side of the IMM. The oxygen consumption results suggested that in *Yl*-mitochondria, there is a physical interaction between NDH2e and the classic respiratory complexes or supercomplexes.

3.3. Y. lipolytica mitochondria contain respiratory supercomplexes resembling those reported in other species

The association of respiratory complexes into supercomplexes has been well documented [12,49]. In addition, oxygen consumption data (Fig. 1) indicated that in *Yl*-mitochondria, NDH2e channels its electrons to the cytochrome pathway, suggesting the existence of a supercomplex. Thus, we decided to search in isolated *Yl*-mitochondria from *Y. lipolytica* for the association of respiratory components into supercomplexes.

LM-solubilised *Yl*-mitochondria exhibited different patterns of complex association depending on the LM/protein ratio. Using BN-PAGE gels, it was observed that at low LM concentrations (0.25 or 0.5 g/g protein), mitochondrial solubilisates contained both individual respiratory complexes and low concentrations of supercomplexes V_2 and $I–III_2$ (result not shown). However, in these conditions complex solubility was poor, so a higher LM/protein ratio (2.0 g/g) was used, where no supercomplex formation was detected (Fig. 2A). By contrast, digitonin-solubilised *Yl*-mitochondria (4.0 g Dig/g protein) revealed the bands corresponding to the individual complexes plus a number of high molecular mass species, suggestive of the presence of different supercomplexes (Fig. 2A).

The complex composition in each band was identified using different methods. Among these was the measurement of in-gel activities. In-gel NADH:NBT oxidoreductase activity (Fig. 2B) was revealed in several bands. In *Yl*-mitochondria LM-solubilised mitochondria two well defined purple bands were detected probably corresponding to complex I and to a NADPH dehydrogenase known as the Old Yellow Enzyme (Fig. 2B). The identity of this NADPH dehydrogenase, marked with an asterisk in Fig. 2B, was determined by mass spectrometry (Fig. 2B; also see Fig. 6 and Table 3). In digitonin-solubilised *Yl*-mitochondria (Fig. 2B), the same two bands were observed and in addition two species with high MWs were detected, probably corresponding to $I–III_2$ and $I–III_2–IV_4$ (Fig. 2B and see below). This is in agreement with the NADH:NBT oxido-reductase

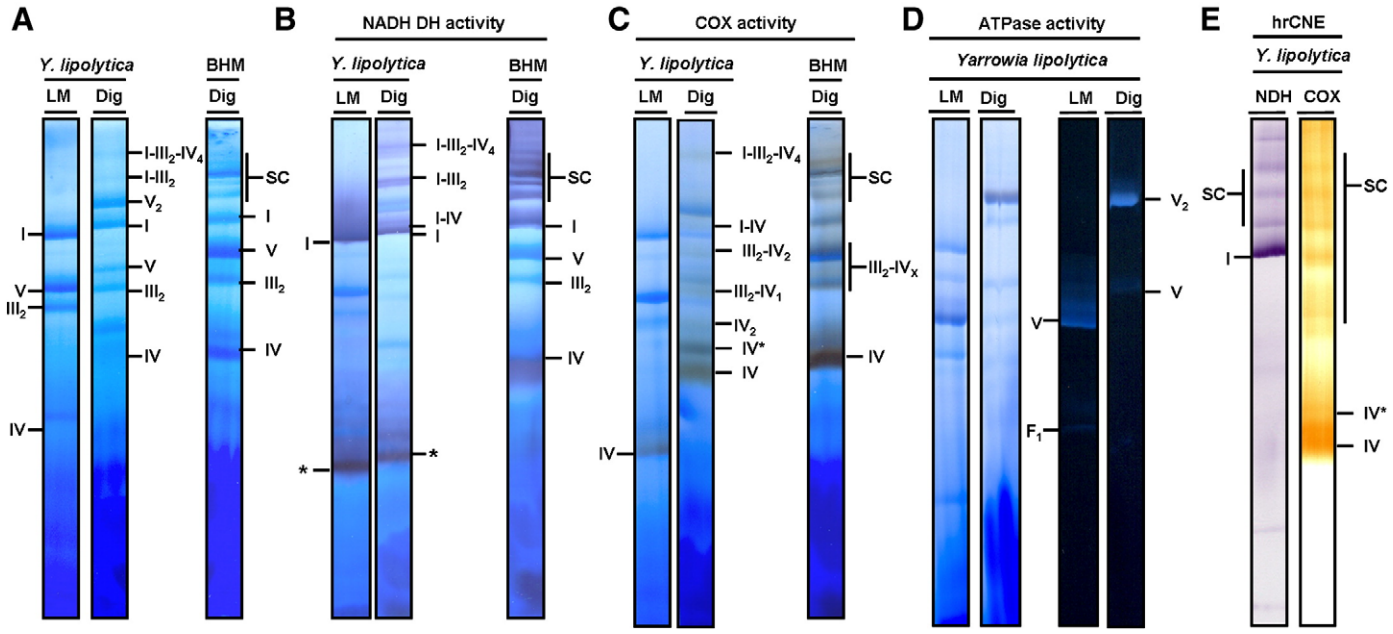

Fig. 2. Respiratory complexes and supercomplexes from solubilised mitochondria from *Y. lipolytica*. Isolated mitochondria were solubilised with the indicated detergent: digitonin (Dig) at 4.0 g/g protein or LM at 2.0 g/g protein. (A) solubilisates were resolved by BN-PAGE in a 4–12% polyacrylamide gradient gel. (B) in-gel NADH-dehydrogenase activity; the BN-gel was incubated in the presence of 1 mM NADH and 0.5 mg/ml Nitro blue tetrazolium chloride (NBT). (C) cytochrome *c* oxidase (COX) in-gel activity. The BN-gel was incubated with diaminobenzidine and cytochrome *c*. (D) BN-gel and detection of in-gel ATPase activity. The BN-gel was incubated with 35 mM Tris, 270 mM glycine, 0.2% $Pb(NO_3)_2$, 14 mM $MgSO_4$ and 8 mM ATP (pH 8.4). Nomenclature used for *Y. lipolytica* mitochondria: I, II, III, IV, V, were the corresponding mitochondrial complexes. Supercomplexes were: I–V; $I–III_2$ and $I–III_2–IV_4$, $III_2–IV_1$ and $III_2–IV_2$ where the stoichiometries are indicated as subindexes; IV*, a high MW form of complex IV, probably artificially generated during BN-PAGE [53]; V_2, complex V dimer. For beef heart mitochondria (BHM): SC, supercomplexes $I–III_2–IV_{0–4}$ as described in [5].

activity band pattern revealed from digitonin-treated beef heart mitochondria (BHM), which included the assigned bands for both complex I alone and complex I associated into supercomplexes (Fig. 2B and see below).

The in-gel cytochrome *c* oxidase activity revealed a single band in LM-solubilised *Yl*-mitochondria, which probably was monomeric complex IV (Fig. 2C). By contrast, in digitonin-solubilised *Yl*--mitochondria, we observed complex IV activity in different bands. The estimated MWs of these bands allow to suggest that these are supercomplexes I–IV, $III_2–IV_2$, $III_2–IV$, $I–III_2–IV_4$ and IV_2 (Fig. 2C and see below).

The F_1-F_o-ATP synthase in-gel activity of LM-solubilised *Yl*-mitochondria revealed a complex V monomer plus a smaller band, probably corresponding to free F_1 (Fig. 2D). In digitonin-solubilised mitochondria, one band corresponding to the complex V monomer, plus a second band probably corresponding to the complex V dimer (V_2) were observed (Fig. 2D and see below).

In an attempt to obtain further data on the location of the putative supercomplexes containing either NADH dehydrogenase or cytochrome oxidase activities, avoiding the interference from the blue-stained bands, we performed another set of in-gel activity measurements using high-resolution clear native electrophoresis (hrCNE) (Fig. 2E). In hrCNE, the observed pattern of *Yl*-mitochondria bands was similar to that observed in the blue gels for both NADH dehydrogenase (Fig. 2B) and for cytochrome oxidase (and 2-C). Thus, for either enzymatic activity, a similar band pattern was detected using two different electrophoretic systems.

The MWs of each respiratory complex and supercomplex detected in the digitonin-solubilised *Yl*-mitochondria BN-gels (Fig. 2) were estimated by comparison with the BHM complexes and supercomplexes. To do so, we included in the BN-gels lanes containing digitonin-solubilised BHM (Fig. 2). In BHM, the MWs of the complexes and supercomplexes are well characterized [3,33], so the comparison of the migration distances allowed to estimate the MWs for each *Y. lipolytica* complex and supercomplex (Fig. 2A). Furthermore, the BHM samples were also used to validate the in-gel activity assays of NADH dehydrogenase (Fig. 2B) and cytochrome *c* oxidase (Fig. 2C).

In order to identify the BN-PAGE bands obtained from the LM-solubilised *Yl*-mitochondria, the sample was run in a 2D-SDS-Tricine-PAGE which was silver-stained (Fig. 3A). The polypeptide patterns derived from each complex were characteristic of each assigned complex [3]. To confirm the identity of each respiratory complex from *Y. lipolytica*, the 2D-gel was electrotransferred onto a nitrocellulose membrane and immunoblotted (Fig. 3B). The membrane was decorated with polyclonal antibodies against the iron–sulfur protein from the bovine bc_1 complex and the beta subunit from *Polytomella* sp. ATP-synthase. Also, a monoclonal antibody against yeast COX III was tested (Fig. 3B). The antibody against the iron–sulfur protein from complex III also recognized the 75 kDa subunit of complex I, i.e. an iron–sulfur-containing subunit from complex I [50].

It was decided to further characterize the BN-PAGE bands obtained from LM-solubilised *Yl*-mitochondria by sequencing some of the polypeptides resolved by 2D-gels. To do this, each band: I, V, III_2 and IV from a BN-PAGE gel was cut and subjected to 2D-SDS-Tricine-PAGE. The 2D-gel was transferred onto a PVDF membrane (ProBlott, Applied Biosystems) and the selected bands were cut for N-terminal sequencing by automated Edman degradation (Fig. 3C and Table 1). The sequence obtained for each band (9 to 12 residues) allowed the identification of the following proteins: in the lane assigned for complex I, band IA was the 40 kDa subunit of the NADH-ubiquinone oxido-reductase. In the lane assigned to complex V, the band VA was identified as the gamma subunit from F_1F_o-ATP synthase. In the lane assigned as complex III, bands IIIA and IIIB were the ubiquinol-cytochrome *c* reductase core proteins 1 and 2, respectively. For the lane assigned as complex IV, we identified two bands: IVA was the cytochrome *c* oxidase subunit 2, while IVB was cytochrome *c* oxidase subunit 4. Thus, the results from Fig. 3 and Table 1 provide an unambiguous indication that the complex assignments made in the gels shown in Fig. 2 are correct.

Digitonin-solubilised *Yl*-mitochondria exhibited additional, high molecular mass bands suggestive of the presence of supercomplexes

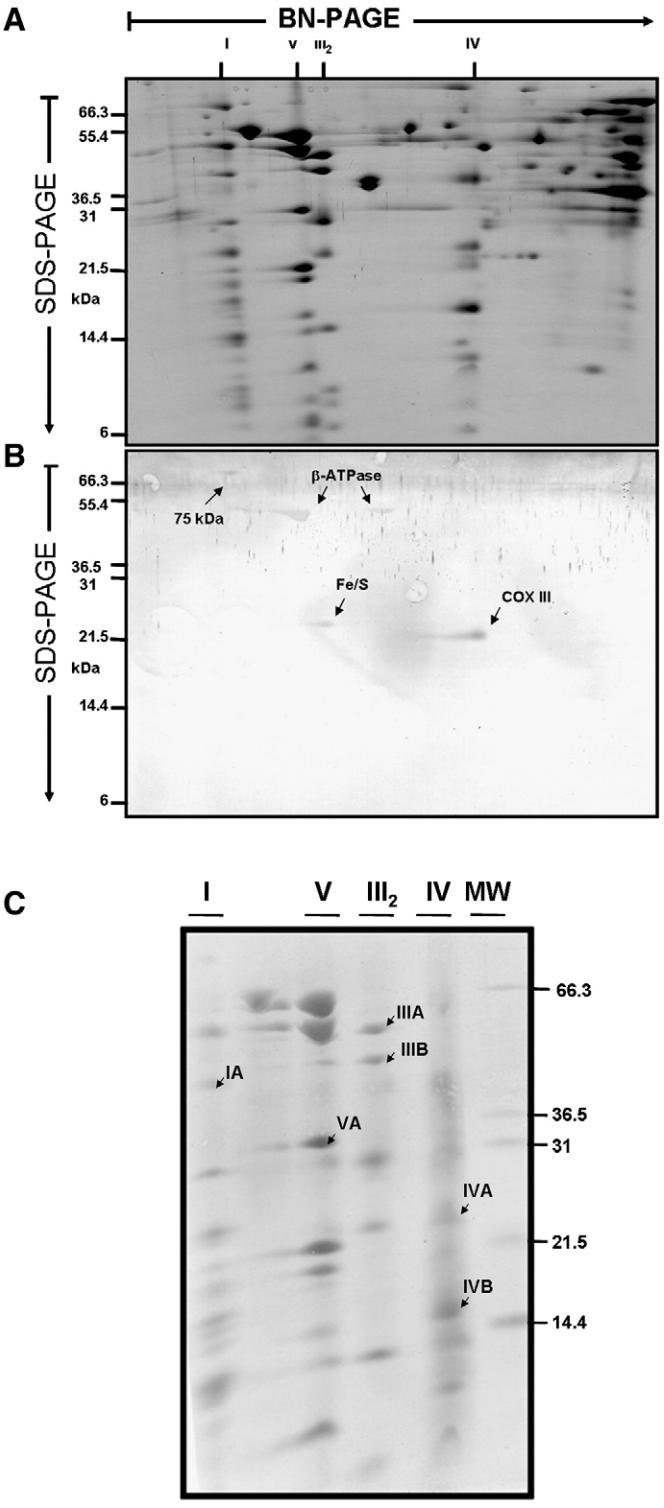

Fig. 3. 2D-SDS-Tricine-PAGE of mitochondrial complexes from *Y. lipolytica*. After BN-PAGE, complete lanes from LM-solubilized mitochondria were excised from the gel and resolved by 2D-SDS-Tricine-PAGE. (A) second-dimension gels stained with Coomasie blue. (B) western blot using antibodies against: *i*) the iron–sulfur protein from the bovine bc_1 complex, which also recognizes the 75 kDa subunit of complex I; *ii*) the beta subunit from the ATPsynthase from *Polytomella* sp; and *iii*) COXIII from *S. cerevisiae*. I, III_2, IV and V, are the respiratory complexes identified. (C) each band from LM lane in the BN-gel from Fig. 2A was excised from the gel and subjected to 2D-SDS-Tricine-PAGE, the resulting gel was electrotransferred to a PDVF membrane. The marked polypeptide bands were cut and analysed by N-terminal sequencing (also see Table 1).

Table 1
Analysed proteins by N-terminal sequencing from the 2D-SDS-Tricine-PAGE (Fig. 3)

Band	Protein name or BLAST homology	Amino terminal sequence	GI protein
IA	NADH-ubiquinone oxidoreductase 39 kDa subunit (NUEM)	NSVESLAQ	50551529
IIIA	Ubiquinol–cytochrome *c* reductase complex core protein 1 precursor	ATTVSX	50545043
IIIBU	Ubiquinol–cytochrome *c* reductase complex core protein 2 precursor	FSTAEAAGVKV	50555522
IVA	Cytochrome *c* oxidase subunit 2 precursor (polypeptide II)	VPVPY	50550873
IVB	COX5A mitochondrial cytochrome-*c* oxidase chain V.A precursor	AHVISTPTL	50555089
	COX4 cytochrome-*c* oxidase chain IV	HKAVKPAE	50553496
VA	ATP3 F1F0-ATPase complex, F1 gamma subunit	ATLREIEMR	50555031

(Fig. 2). The polypeptide pattern of each of these bands was resolved in 2D-SDS-Tricine-PAGE (Fig. 4). The polypeptide composition of the high molecular mass components suggested the presence of supercomplexes I_1–III_2 and I–III_2–IV_4, as the presence of the 75 kDa subunit from complex I and the core proteins from the bc_1 complex was evidenced. We also observed bands probably corresponding to a complex V dimer (V_2) and to a III_2–IV_2 supercomplex (Fig. 4). The SDS-Tricine-PAGE migration pattern in Fig. 4, together with the in-gel activities reported above (Fig. 3) strongly suggests the presence of supercomplexes in *Yl*-mitochondria.

A more quantitative approach to estimating the MW was attempted by analysing the migration distances for the digitonin-solubilised mitochondrial complexes and supercomplexes from both *Y. lipolytica* and BHM (Fig. 2A). First, the logarithm of the MW of each BHM complex and supercomplex was plotted against its migration distance in the gel (Fig. 5). Then, the migration distances from the *Yl*-mitochondria-derived bands were interpolated (Fig. 5). The MW estimates for the yeast complexes and supercomplexes are reported in Table 2. The MWs for complexes I, III and IV were slightly smaller than their BHM counterparts. For complex V, the difference in MW was larger. From the estimated MWs, the in-gel activities, the immunoblotting data and the sequencing of different bands in the gels, the presence of different supercomplexes may be proposed. The supercomplexes we detected in the *Y. lipolytica* BN- and CN-gels were assigned as: I_2, I–IV, I–III_2–IV_4, III_2–IV, III_2–IV_2, IV_2 and V_2.

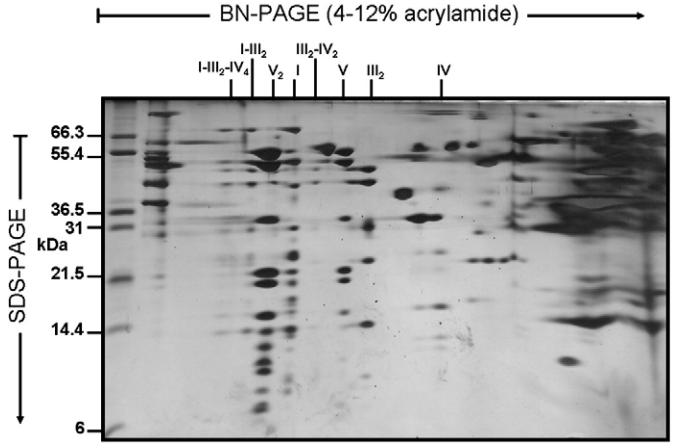

Fig. 4. 2D-SDS-Tricine-PAGE of *Y. lipolytica* mitochondrial complexes and supercomplexes. After BN-PAGE, the lane containing the digitonin solubilised proteins was excised and subjected to 2D-SDS-Tricine-PAGE followed by silver staining. Complex and supercomplex nomenclature as in Fig. 2.

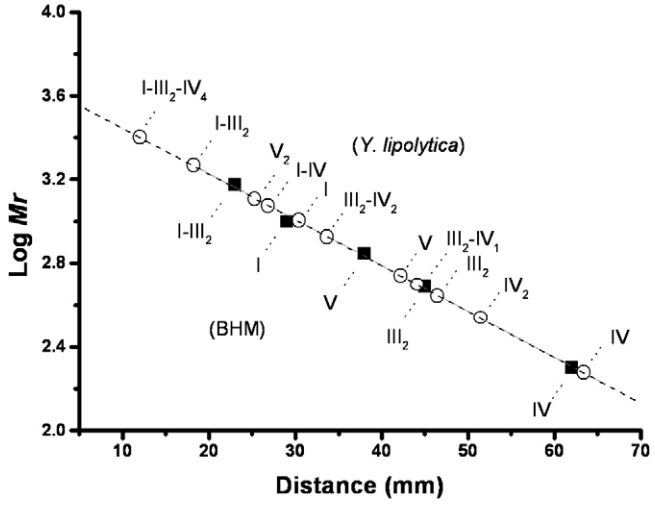

Fig. 5. Molecular mass estimates of the *Y. lipolytica* complexes and supercomplexes. The logarithms of the well-characterized molecular masses of the bovine heart mitochondrial complexes and supercomplex $I–III_2$ (■) were plotted against their migration distance in BN-PAGE (Fig. 2). Then, the migration distances of the *Y. lipolytica* respiratory complexes and supercomplexes (○) were interpolated and their corresponding molecular masses inferred (see values in Table 2).

3.4. When in the external face, but not when in the internal face of the inner mitochondrial membrane, NDH2 is bound to respiratory complexes

The oxygen consumption data indicated that NDH2e channelled its electrons to the cytochrome pathway (Fig. 1), suggesting a physical association with a supercomplex III–IV. In addition, the *Δnubm* mutant, with an inactive complex I plus the matrix-redirected NDH2 (NDH2i) probably lost this association, as it donated electrons either to the cytochrome pathway or to AOX. Thus, in order to determine whether NDH2e associates to the cytochrome complexes, digitonin-solubilised *Yl*-mitochondria were electrophoresed in a CN-gel and evaluated for NADH dehydrogenase and cytochrome *c* oxidase in-gel activities (Fig. 6A). As expected, the electrophoretic pattern in CN-PAGE differs from the one obtained with BN-PAGE, since in the former case the electrophoretic mobilities of proteins are given by their mass and intrinsic charge [37,51]. In addition, a non-associated native NDH2e was not expected to enter the gels due to its high isoelectric point of 8.45, unless it was dragged in by another associated protein. The mutant NDH2i did not have this problem as the deletion of 101 aminoacids resulted in a predicted isoelectric point of 6.0.

In wild-type *Yl*-mitochondria, three NADH dehydrogenase activity bands were detected. Mass spectrometry analyses of these bands indicated that heaviest band was complex I (see below) and the third band was a NADPH dehydrogenase (Table 3). Thus, the second band was the only one where there was a possibility of finding NDH2e in association with a cytochrome complex. In the *Δnubm* mutant, the heaviest band disappeared, further suggesting that this was complex I, while the other two bands were still present. In addition, in *Δnubm* an extra band appeared in the bottom of the gel which was identified as NDH2; most probably this was the redirected NDH2i. Once all other bands were identified and discarded, the second band from the wild-type strain, also detected in *Δnubm*, was the only candidate where NDH2e might be present in association to a respiratory complex. In order to test this, a different lane of the same gel was stained for cytochrome *c* oxidase in-gel activity: both in the WT and in the *Δnubm* mutant a single, broad band exhibiting cytochrome *c* oxidase activity was obtained (Fig. 6A). This band migrated the same distance as the band exhibiting NADH dehydrogenase activity, suggesting NDH2e-cytochrome *c* oxidase association and explaining the slow migration of NDH2e as compared to NDH2i. When both complex IV and complex III were revealed, it was observed that complex III exhibited a slightly lower mobility (Fig. 6A, last lane, labelled as Cyt), again suggesting that NADH2e associated specifically to complex IV. Further characterization of the proteins in the CN-gel was obtained by running a 2D-SDS-Tricine-PAGE for the wild-type strain (Fig. 6B). All the signature polypeptides for complexes V_2, I, III, V and IV were detected at the expected positions. In addition, the comigration of NDH2e and complex IV was observed (Fig. 6B). This comigration was further evidenced by immunoblotting of this gel with anti-NDH2e and anti-COX III antibodies (Fig. 6B lower panel). In order to further identify the lower molecular mass band detected in the mutant strain, the band from the CN-gel was cut, transferred and immunoblotted against NDH2e antibodies. In the mutant, but not in the wild-type strain, a positive staining indicated that this band is a freely migrating NDH2, most probably NDH2i (Fig. 6C).

The absence of a freely migrating NDH2e in the lane corresponding to the LM-solubilised wild-type *Yl*-mitochondria (Fig. 6A and C) suggested that the interaction between NDH2e and the cytochrome pathway was strong enough to resist the LM-mediated dissociation. Thus, it was decided to analyse whether NDH2e and the cytochrome complex(es) migrated together in the LM-solubilised organelles. To do this, mass spectrometry was performed on two bands of interest (Table 3): one band was cut from the wild-type/LM lane (band X), at the height where NADH dehydrogenase and cytochrome *c* oxidase activities were detected in all gels both by activity (Fig. 6A) and by immunoblotting (Fig. 6B). The second cut was made at a band exhibiting NADH dehydrogenase activity in all gels (band Y) (Fig. 6A). Band X contained various proteins from complex IV, complex III and complex V, in addition NDH2e was detected. By contrast, band Y contained NAD(P)H dehydrogenase explaining the activity detected, plus glycerol-3-dehydrogenase and a complex II subunit, the 70 kDa flavoprotein-ubiquinone oxido-reductase (Table 3).

Further evidence of the association of NDH2e with cytochrome oxidase was obtained when a LM-solubilisate of *Yl*-mitochondria was loaded onto a DEAE-Sepharose column that separates the yeast oxidative phosphorylation complexes [52]. When protein was eluted by a NaCl gradient, the protein concentration elution profile exhibited one major peak followed by a shoulder containing smaller amounts of protein. When the eluted fractions were assayed for enzymatic activities it was observed that those from the large protein peak contained complex I plus complex V, as evidenced by measurements of the NADH dehydrogenase (Fig. 7B) and ATPase (result not shown) activities. By BN-PAGE, it was observed that these fractions contained complex I and complex V (result not shown). The elution fractions from the shoulder appearing at the end of the protein peak exhibited cytochrome *c* oxidase activity plus a second peak of NADH dehydrogenase activity (Fig. 7B). In order to detect whether NADH2e and COX were present in the fractions 72 to 86, corresponding to the second activity peak, we immunoassayed for NADH2e and for COXIII and we detected both proteins (Fig. 7C). In contrast, the fractions

Table 2
Estimated masses of *Yarrowia lipolytica* complexes and supercomplexes by BN-PAGE

Complexes	Calculated Mr (kDa)	Supercomplexes[a]	Calculated Mr (kDa)	Expected Mr (kDa)
I	960±50	I–III2	1750±124	1418
II	ND	I–III2–IV4	2339±69	2174
III2	458±16	I–IV	1217±46	1149
IV	189±9.9	III2–IV2	858±30	826
V	543±10	V2	1231±70	1086

I–V, respiratory complexes I–V;
III2, complex III dimer.
ND, not determined.
Expected Mr corresponds to the calculated values obtained from the independent complexes.
[a] Subscript numbers indicate the number of copies of each complex in the supercomplex.

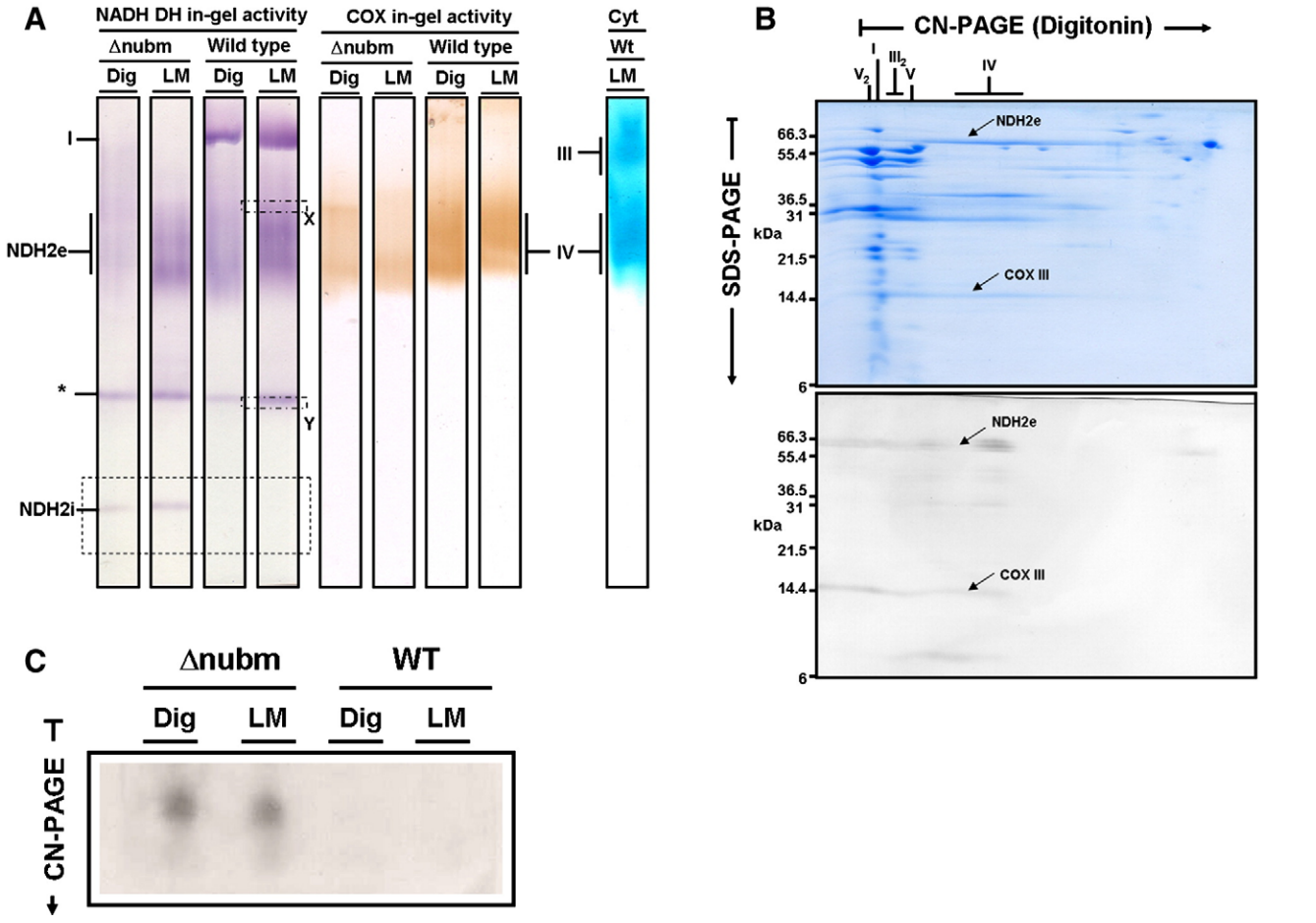

Fig. 6. Interaction between the external NADH dehydrogenase and the cytochrome pathway. (A) mitochondrial proteins solubilized with digitonin (Dig) were subjected to CN-PAGE followed by in-gel staining for either NADH dehydrogenase or cytochrome *c* oxidase activities. Two bands, labelled X and Y were cut and subjected to LC-MS/MS; the results are shown in Table 3. (B) 2D-SDS-Tricine-PAGE stained with Coomasie blue identifying each complex as indicated. (Panel C) the 2D-gels were electrotransferred onto nitrocellulose membrane for western blotting. The membrane was decorated with a polyclonal antibody against the *Y. lipolytica* NDH2e and with a monoclonal antibody against COXIII of *S. cerevisiae*. (D) Western blot of a section of the CN-gel (marked as NDH2i in a rectangle in panel A) decorated with the anti-NDH2 antibody.

eluting before or after the second activity peak were negative for both antibodies (Fig 7C). Also, in a BN-PAGE of the fractions from the second peak we did not find evidence of the presence of complex I (result not shown). The coelution of complex IV and NDH2e is another indication that these proteins associate. Again, it is interesting to note that the high isoelectric point of NDH2e would have resulted in non-

Table 3
Proteins identified by LC-MS/MS analysis contained in the indicated bands from the CN gel (Fig. 6)

Band		Protein name or BLAST homology	Accession no.	gI protein	MW* (kDa)
X	IV	Cytochrome *c*-oxidase chain V.A	XP_504953	50555089	18.9
		Cytochrome *c*-oxidase chain IV	XP_504159	50553496	17.4
		Cytochrome *c*-oxidase chain VI	XP_503766	50552712	17.1
		Cytochrome *c* oxidase subunit II	Q9B6D5	54035892	27.6
	***	YlNDH2 [*Yarrowia lipolytica*]	XP_505856	50556896	65.8
		malate dehydrogenase	XP_502909	50550873	35.9
	III	COB protein [*Yarrowia lipolytica*]	NP_075443	12718941	43.7
		Ubiquinol:cytochrome-*c* reductase chain II	XP_505169	50555522	44.2
		Ubiquinol:cytochrome-*c* reductase subunit 7	XP_504755	50554693	14.6
	V	F1F0-ATPase complex α subunit	XP_504936	50555055	58
		ATPsynthase β chain mitochondrial precursor	XP_500475	50545874	59.7
		ATP synthase oligomycin sensitivity conferring protein mitochondrial precursor	XP_502751	50550557	17.1
		ATP3 F1F0-ATPase complex, F1 gamma subunit	XP_504924	50555031	31
		ATP synthase δ chain mitochondrial precursor	XP_503135	50551323	17.8
		ATP4 F1F0-ATPase complex, F0 subunit B singleton	XP_505657	50556498	24
Y		NAPDH dehydrogenase (old yellow enzyme)	XP_500567	50546080	46.2
		Electron transfer flavoprotein-ubiquinone oxidoreductase mitochondrial precursor	XP_501844	50548749	71.7
		Glycerol-3-phosphate dehydrogenase	XP_50086	50546785	67.5

III, Ubiquinol:cytochrome *c* oxidoreductase subunits.
IV, Cytochrome *c* oxidase subunits.
V, ATPsynthase subunits.
***External NADH dehydrogenase (NDH2e).
*Predicted protein mass.

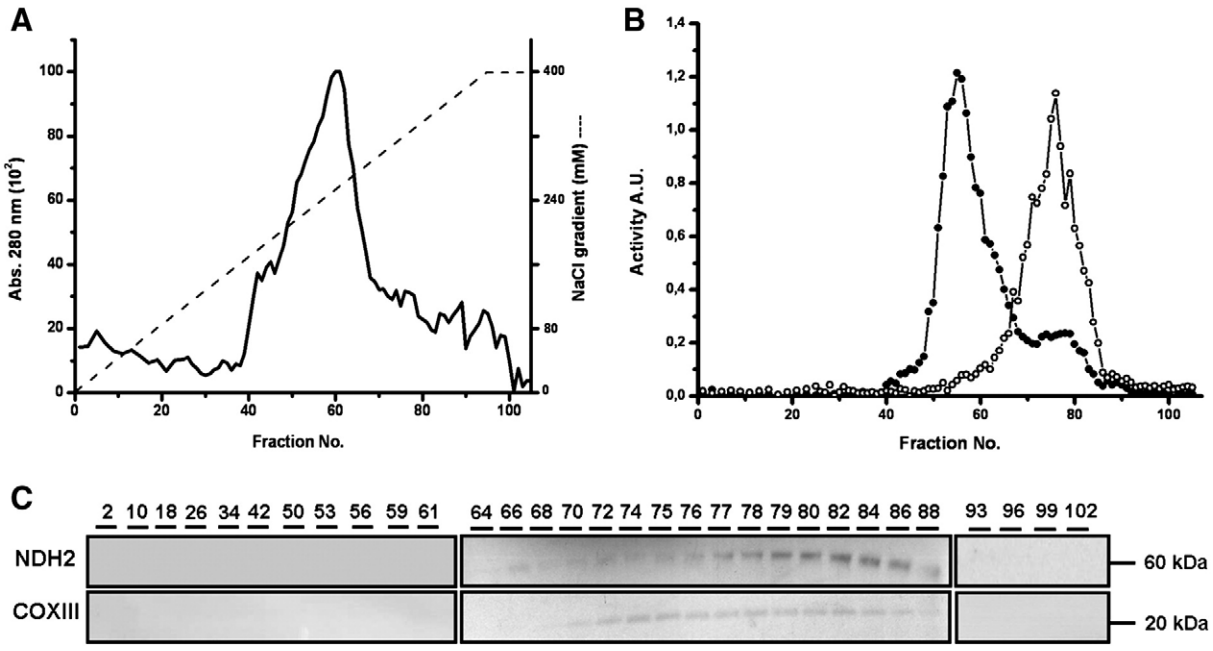

Fig. 7. Ion exchange chromatography elution profile of LM-solubilised *Y. lipolytica* mitochondria. Yeast mitochondrial membranes were solubilised with 2 mg LM/mg protein and loaded onto a DEAE-Sepharose column. After washing with 1 mM $MgSO_4$, 50 mM Tris, pH 8.0, fractions were eluted with a NaCl gradient (0–400 mM) as depicted (discontinuous line) in panel A. The elution pattern of the proteins not retained during the washing step is not shown. (A) Protein concentration in each fraction, determined spectrophotometrically at 280 nm. (B) NADH dehydrogenase activity (●) and cytochrome oxidase activity (○) of each fraction measured spectrophotometrically in ELISA plates. (C) Western blotting of selected fractions from the elution profile to detect NDH2e (at 60 kDa) or CoxIII (at 20 kDa).

association of this enzyme to the column, unless it was retained as a complex with another protein.

The oxymetry, the native gel and the chromatography data suggested that NDH2e was associated to the cytochrome pathway, probably in tight association with cytochrome *c* oxidase. The proposed interaction would be specific, as NDH2e seems to associate with complex IV at putative sites located on the external face of the IMM that are not accessible to the redirected NDH2i; in addition, it is a rather strong interaction, as it does not seem to be disrupted by the presence of a LM concentration reported to dissociate supercomplexes [51].

4. Discussion

The detection of supramolecular complex associations has led to new ideas on the physiology, structure and function of the respiratory chain [12,13]. It has been proposed that supercomplexes promote substrate-channelling and sequestering of reactive oxygen species [53]. Also, it has been reported that supramolecular association results in structure stabilization of labile, multi-subunit complexes [54]. Different association patterns of complexes I, III and IV have been observed by BN-PAGE, suggesting the existence of a large supercomplex catalyzing all respiratory reactions i.e. the "respiratory string" [4]. In plants, supercomplexes I_1–III_2–IV_1 [5] and I_1–III_2 [6] have been observed, while in *S. cerevisiae* a supercomplex III_2–IV_2 has been detected [7]. By contrast, in mitochondria from *Y. lipolytica*, supercomplexes have not been detected [38,54]. In this regard, it was proposed that the structure of complex I from *Y. lipolytica* is stable enough to survive without associating to other complexes [55]. Another proposal was that complex–complex associations in *Y. lipolytica* are more labile than those in plants or mammalians [38]. In agreement with the latter proposition, we could not detect supercomplexes in frozen–thawed mitochondria [result not shown]. However, when freshly-prepared mitochondria were solubilised immediately after isolation, we were able to gather evidence of the presence of a complex V dimer and the respiratory supercomplexes I_1–III_2, I_1–III_2–IV_4, I–IV, III_2–IV and III_2–IV_2. The presence of these supercomplexes has been reported in mitochondria from other fungi [56]. In regard to the high tendency of the *Y. lipolytica* supercomplexes to dissociate, it would be interesting to determine whether supercomplex formation/dissociation is regulated by the metabolic requirements of the cell, and whether the phase of growth is critical for the formation of respiratory supercomplexes as proposed for *P. anserina* [57].

In plants and many fungi, mitochondrial alternative oxidoreductases provide various possibilities for electrons to reach oxygen. External NADH dehydrogenases (NDH2e) shuttle electrons from the cytoplasm to the respiratory chain [22], while internal NADH dehydrogenases (NDH2i) catalyze electron transfer from the matrix dehydrogenases to oxygen. In some yeast, NDH2e and NDH2i may substitute for complex I, as is the case in *S. cerevisiae* [58]. Another possible physiological role for NDH2i is illustrated by *Neurospora crassa* mitochondria which contain both NDH2i and complex I. It has been observed that in the early logarithmic phase of growth, *N. crassa* mitochondria use NDH2i preferentially [59]. In this regard, it has been proposed that although NDH2i produces a lower ATP/O ratio, this is compensated by the large increase in the rate of oxygen uptake leading to increased ATP production. Also, during early growth *N. crassa* would save metabolic energy by building a monomeric, low molecular mass NDH2i instead of the costly 40-subunit complex I [59,60].

In regard to mitochondrial AOX, its activation by α-keto acids has been reported in plants [61,62]. The activated AOX acts in parallel to the cytochrome pathway, i.e. AOX competes for electrons with complex III, and is not just an overflow valve [63]. In fungi no activation seems to be required [64]. Indeed, in *Y. lipolytica* mitochondria the pyruvate/malate-supported rate of oxygen consumption was only partially inhibited by KCN, indicating that the complex I-quinone-AOX pathway was active in the absence of effectors (Fig. 1A).

The lack of proton pumping activity by NDH2s and AOX may be a problem when these enzymes coexist in the same organelle, since the risk of a futile electron pathway emerges, i.e. the transfer of electrons to

oxygen following the path NDH2e-quinone-AOX would not add to the proton gradient [26]. Thus, where NDH2s and AOX coexist, their function has to be tightly controlled, at least during growth or under high energy demand. Two possibilities for regulation arise: the first would be the direct association between complex I and AOX. In this regard, *P. anserina*, where complex III is necessary for the assembly/stability of complex I, the supercomplex I_2–III_2 channels its electrons to AOX [27]. However, a physical association between AOX and supercomplex I_2–III_2 could not be detected in *P. anserina* [27]. In agreement with these results, in *Y. lipolytica* mitochondria we did not detect association of AOX with other respiratory enzymes (result not shown).

The second possibility guaranteeing proton pumping is the association of NDH2(s) to complex III or to supercomplex III–IV. In *Y. lipolytica* we did collect evidence indicating that there is an association of NDH2e to complex IV; then, the association of complex IV into an III–IV supercomplex would result in association of the full pathway. NDH2e association to the cytochrome pathway was suggested by the finding that the NDH2e-supported consumption of oxygen was fully inhibited by KCN while PG did not exhibit effects, i.e. electrons from NDH2e were channeled exclusively to the cytochrome pathway (Fig. 1A). By contrast, electrons coming from complex I seemed to access another, non-localized pool of quinone, reducing either the KCN-sensitive complex IV or the PG-sensitive AOX (Fig. 1A). NDH2e-dependent channelling of electrons is at variance with results in a published report indicating that in the presence of antimycin-A, electrons were accepted by the alternative pathway [65]. Our failure to detect this redirection of electrons may be due to the growth stage of cells used by each group: in the aforementioned report stationary phase cells were used [65], while our study was conducted with mitochondria obtained from cells in the logarithmic growth phase.

NDH2e association to the cytochrome pathway was also detected in CN-gels, where a band containing NDH2e together with subunits of complex IV was observed by in-gel NADH dehydrogenase and cytochrome *c* oxidase activities (Fig. 6A) and by immunoblotting (Fig. 6C). In support of the suggested association between cytochrome-*c*-oxidase and NDH2e, these two enzymes coeluted when a mitochondrial homogenate was subjected to ion exchange chromatography. In this regard, it must be noted that the predicted isoelectric point for NDH2e is 8.45, which should have resulted in exclusion of this protein from the CN gels or non-retention by the DEAE-Sepharose column unless another associated protein dragged it into the gel or retained it in the column. This is not the case for NDH2i, where 101 aminoacid residues have been deleted [24], resulting in a predicted isoelectric point of 6.0.

Our results suggest that in the logarithmic growth phase, *Y. lipolytica* mitochondria contain a supercomplex formed by NDH2e, complex III and complex IV. This is in agreement with the reports on the existence of III_2–IV_2 supercomplexes in *S. cerevisiae* [7] and with the supercomplexes detected under our experimental conditions (Figs. 2 and 4). In addition, the NDH2e-cytochrome *c* oxidase association is probably quite strong, as we could not detect evidence of a non-associated NDH2e even in the presence of LM (2.0 g/g protein) (Fig. 3C), a concentration that usually disrupts cytochromic supercomplexes (Figs. 2 and 3).

In the *Δnubm* mutant, the redirected NDH2i was detected running independently of the cytochrome complexes, suggesting that the putative interaction between NDH2e and the cytochrome complexes involves specific protein domains in the IMM that are exposed towards the intermembrane space. These domains would not be available to the redirected NDH2i. It would be highly desirable to identify the actual NDH2e binding site in the cytochrome complexes. Another possibility is that the 101 residues that were deleted from NDHi were critical for the proposed interaction.

We tested the presence of NDH2e association to supercomplexes only in the logarithmic growth phase of the yeast. However, it may be speculated that in conditions where large amounts of ATP are needed (the logarithmic phase), mitochondria have to be highly coupled. In contrast, in conditions such as the stationary phase, where less ATP is needed, a certain degree of uncoupling would be desirable, i.e. the NDH2e dissociation from the cytochrome complexes, and its functional association with AOX would be advantageous. An alternative electron sink for most mitochondria would be the permeability transition, as is the case of mammals, plants and *S. cerevisiae* [66–68]. However, *Y. lipolytica* does not seem to have a transition pore [69; unpublished data] and thus the dissociation of NDH2e resulting in freedom to feed electrons to AOX would probably constitute an alternate mechanism to maintain a high rate of oxygen consumption.

To our knowledge, this is the first report indicating that there are respiratory supercomplexes in *Y. lipolytica* mitochondria, and also the first time evidence is provided suggesting the association of an alternative respiratory component (NDH2e) to the major cytochrome complexes.

Acknowledgements

Dr. Stefan Kerscher and Dr. Ulrich Brandt, kindly provided the *Y. lipolytica* strains and specific antibodies against *Yl*NDH2e. We thank Dr. Gilles Peltier for the gift of the *At*NDH2 antibody. The expert technical help of Ramón Méndez-Franco is acknowledged. We are grateful to Lorena Morales Sáinz, who participated in the early phase of the project. We also thank Dr. Xochitl Pérez-Martínez for her critical review of the paper. Rocío Romualdo-Martínez helped to type the manuscript. S.G.-C. is a CONACyT fellow. Partially supported by grants 79989 (SU) and 56619 (DGH) from CONACyT, and IN216206 (SU) and IN218705-3 (DGH) from DGAPA, UNAM.

References

[1] Y. Hatefi, The mitochondrial electron transport and oxidative phosphorylation system, Ann. Rev. Biochem. 54 (1985) 1015–1069.
[2] D.G. Nicholls, S.J. Ferguson, Bioenergetics 3, Academic Press, London, 2002.
[3] H. Schägger, K. Pfeiffer, The ratio of oxidative phosphorylation complexes I–V in bovine heart mitochondria and the composition of respiratory chain super complexes, J. Biol. Chem. 276 (2001) 37861–37867.
[4] I. Wittig, R. Carrozzo, F.M. Santorelli, H. Schägger, Supercomplexes and supcomplexes of mitochondrial oxidative phosphorylation, Biochim. Biophys. Acta 1757 (2006) 1066–1072.
[5] E. Schäfer, N.A. Dencher, J. Vonck, D.N. Parcej, Three-dimensional structure of the respiratory chain supercomplex $I_1III_2IV_1$ from bovine heart mitochondria, Biochemistry 46 (2007) 12579–12585.
[6] N.V. Dudkina, H. Eubel, W. Keegstra, E.J. Boekema, H.P. Braun, Structure of a mitochondrial supercomplex formed by respiratory-chain complexes I and III, Proc. Natl. Acad. Sci. U. S. A. 102 (2005) 3225–3229.
[7] J. Heinemeyer, H.P. Braun, E.J. Boekema, R. Kouil, A structural model of the cytochrome *c* reductase/oxidase supercomplex from yeast mitochondria, J. Biol. Chem. 282 (2007) 12240–12248.
[8] F. Minauro-Sanmiguel, S. Wilkens, J.J. García, Structure of dimeric mitochondrial ATP synthase: novel F_0 bridging features and the structural basis of mitochondrial cristae biogénesis, Proc. Natl. Acad. Sci. U. S. A. 102 (2005) 12356–12358.
[9] G. Arselin, M.F. Giraud, A. Dautant, J. Vaillier, D. Brèthes, B. Coulary-Salin, J. Schaeffer, J. Velours, The GxxxG motif of the transmembrane domain of subunit e is involved in the dimerizatio/oligomerization of the yeast ATP synthase complex in the mitochondrial membrane, FEBS J. 270 (2003) 1875–1884.
[10] R. van Lis, D. González-Halphen, A. Atteia, Divergence of the mitochondrial electron transport chains from the green alga *Chlamydomonas reinhardtii* and its colorless close relative *Polytomella* sp, Biochim. Biophys. Acta 1708 (2005) 23–34.
[11] E.J. Boekema, H.P. Braun, Supramolecular structure of the mitochondrial oxidative phosphorylation system, J. Biol. Chem. 282 (2007) 1–4.
[12] H. Schägger, Respiratory chain supercomplexes, IUBMB Life 52 (2001) 119–128.
[13] H. Eubel, J. Heinemeyer, S. Sunderhaus, H.P. Braun, Respiratory chain supercomplexes in plant mitochondria, Plant Physiol. Biochem. 42 (2004) 937–942.
[14] T. Joseph-Horne, D.W. Hollomon, P.M. Wood, Fungal respiration: a fusion of standard and alternative components, Biochim. Biophys. Acta 1504 (2001) 179–195.
[15] B.T. Storey, The respiratory chain of plant mitochondria. XIII: point of interaction of the alternative oxidase with the respiratory chain, Plant Physiol. 58 (1976) 521–525.
[16] D.P. Maxwell, Y. Wang, L. McIntosh, The alternative oxidase lowers mitochondrial reactive oxygen production in plant cells, Proc. Natl. Acad. Sci. U. S. A. 96 (1999) 8271–8276.
[17] A.L. Moore, J.N. Siedow, The regulation and nature of the cyanide-resistant alternative oxidase of plant mitochondria, Biochim. Biophys. Acta 1059 (1991) 121–140.

[18] H. Boumans, L. Grivell, J.A. Berden, The respiratory chain in yeast behaves as a single functional unit, J. Biol. Chem. 273 (1998) 4872–4877.
[19] S. Kerscher, J.G. Okun, U. Brandt, A single external enzyme confers alternative NADH:ubiquinone oxidoreductase activity in *Yarrowia lipolytica*, J. Cell Sci. 112 (1999) 2347–2354.
[20] J.N. Siedow, A.L. Umbach, The mitochondrial cyanide-resistant oxidase: structural conservation amid regulatory diversity, Biochim. Biophys. Acta 1459 (2000) 432–439.
[21] A.G. Medentsev, V.K. Akimenko, Development and activation of cyanide-resistant respiration in the yeast *Yarrowia lipolytica*, Biochemistry (Mosc.) 64 (1999) 945–951.
[22] S. Kerscher, S. Dröse, K. Zwicker, V. Zickermann, U. Brandt, *Yarrowia lipolytica*, a yeast genetic system to study mitochondrial complex I, Biochim. Biophys. Acta 1555 (2002) 83–91.
[23] S. Kerscher, Diversity and origin of alternative NADH:Ubiquinone oxidoreductases, Biochim. Biophys. Acta 1459 (2000) 274–283.
[24] S. Kerscher, A. Eschemann, P. Okun, U. Brandt, External alternative NADH: Ubiquinone oxidoreductase redirected to the internal face of the inner mitochondrial membrane rescues complex I deficiency in *Yarrowia lipolytica*, J. Cell Sci. 114 (2001) 3915–3921.
[25] V.K. Akimenko, N.P. Golovchenko, A.G. Medentsev, The absence of energy conservation coupled with electron transfer via the alternative pathway in cyanide-resistant yeast mitochondria, Biochim. Biophys. Acta 545 (1979) 398–403.
[26] A. Veiga, J.D. Arrabaça, F. Sansonetty, P. Ludovico, M. Côrte-Real, M.C. Lourerio-Dias, Energy conversion coupled to cyanide-resistant respiration in the yeast *Pichia membranifaciens* and *Debaryomyces hansenii*, FEMS Yeast Res. 3 (2003) 141–148.
[27] F. Krause, C.Q. Scheckhuber, A. Werner, S. Rexroth, N.H. Reifscheider, N.A. Dencher, H.D. Osiewacz, Supramolecular organization of cytochrome *c* oxidase- and alternative oxidase-dependent respiratory chains in the filamentous fungus *Podospora anserine*, J. Biol. Chem. 279 (2004) 26453–26461.
[28] H. Eubel, L. Jänsch, H.P. Braun, New insights into the respiratory chain of plant mitochondria. Supercomplexes and a unique composition of complex II, Plant Physiol. 133 (2003) 274–286.
[29] F.M. Pérez-Campo, A. Domínguez, Factors affecting the morphogenetic switch in *Yarrowia lipolytica*, Curr. Microbiol. 43 (2001) 429–433.
[30] A. Peña, M.Z. Piña, E. Escamilla, E. Piña, A novel method for the rapid preparation of coupled yeast mitochondria, FEBS Lett. 80 (1977) 209–213.
[31] A.G. Gornal, C.J. Bardavill, M.M. David, Determination of serum protein by means of the biuret reaction, J. Biol. Chem. 177 (1949) 751–760.
[32] H. Low, I. Vallin, Succinate-linked diphosphopyridine nucleotide reduction in submitochondrial particles, Biochim. Biophys. Acta 69 (1963) 361–374.
[33] I. Wittig, H.P. Braun, H. Schägger, Blue native PAGE, Nat. Protoc. 1 (2006) 418–428.
[34] R.W. Estabrook, Mitochondrial respiratory control and the polarographic measurements of ADP:O ratios, Methods Enzymol. 10 (1967) 41–47.
[35] H. Schägger, Blue native gels to isolate protein complexes from mitochondria, Methods Cell Biol. 65 (2001) 231–244.
[36] H. Schägger, G. von Jagow, Native electrophoresis for isolation of mitochondrial oxidative phosphorylation protein complexes, Methods Enzymol. 260 (1995) 190-203.
[37] I. Wittig, H. Schägger, Advantages and limitations of clear-native PAGE, Proteomics 5 (2005) 4338–4346.
[38] I. Wittig, M. Karas, H. Schägger, High resolution clear native electrophoresis for in-gel functional assays and fluorescence studies of membrane protein complexes, Mol. Cell. Proteomics 6 (2007) 1215–1225.
[39] H. Schägger, G. von Jagow, Blue native electrophoresis for isolation of membrane protein complexes in enzymatically active form, Anal. Biochem. 199 (1991) 223–231.
[40] E. Zerbetto, L. Vergani, F. Dabbeni-Sala, Quantification of muscle mitochondrial oxidative phosphorylation enzymes via histochemical staining of blue native polyacrylamide gels, Electrophoresis 18 (1997) 2059–2064.
[41] O. Juárez, G. Guerra, F. Martínez, J.P. Pardo, The mitochondrial respiratory chain of *Ustilago maydis*, Biochim. Biophys. Acta 1658 (2004) 244–251.
[42] P.E. Thomas, D. Ryan, W. Levin, An improved staining procedure for the detection of the peroxidase activity of the cytochrome P-450 on sodium dodecyl sulfate polyacrilamide gels, Anal. Biochem. 75 (1976) 168–176.
[43] M. Vázquez-Acevedo, P. Cardol, A. Cano-Estrada, M. Lapaille, C. Remacle, D. González-Halphen, The mitochondrial ATP synthase of chlorophycean algae contains eight subunits of unknown origin envolved in the formation of an atypical stator-stalk and in the dimerization of the complex, J. Bioenerg. Biomembr. 38 (2006) 271–282.
[44] A. Garofano, A. Eschemann, U. Brandt, S. Kerscher, Substrate-inducible versions of internal alternative NADH: ubiquinone oxidoreductase from *Yarrowia lipolytica*, Yeast 23 (2006) 1129–1136.
[45] L. Bernard, C. Desplats, F. Mus, S. Cuiné, L. Coumac, G. Peltier, *grobacterium tumefaciens* type II NADH dehydrogenase. Characterization and interactions with bacterial and thylakoid membranes, FEBS J. 273 (2006) 3625–3637.
[46] M. Vázquez-Acevedo, A. Antaramian, N. Corona, D. González-Halphen, Subunit structures of purified beef mitochondrial cytochrome bc_1 complex from liver and heart, J. Bioenerg. Biomembr. 25 (1993) 401–410.
[47] A. Atteia, G. Dreyfus, D. González-Halphen, haracterization of the alpha and beta-subunits of the F0F1-ATPase from the alga *Polytomella* spp., a colorless relative of *Chlamydomonas reinhardtii*, Biochim. Biophys. Acta 1320 (1997) 275–284.
[48] R.T. Wedding, C.C. McCready, J.L. Harley, Inhibition and stimulation of the respiration of *Arum* mitochondria by cyanide and its relation to the coupling of oxidation and phospholylation, New Phytol. 72 (1973) 1–13.
[49] H. Schägger, K. Pfeiffer, Supercomplexes in the respiratory chains of yeast and mammalian mitochondria, EMBO J. 19 (2000) 1777–1783.
[50] U. Brandt, Energy converting NADH:Quinone oxidoreductase (Complex I), Annu. Rev. Biochem. 75 (2006) 69–92.
[51] H. Schägger, W.A. Cramer, G. von Jagow, Analysis of molecular masses and oligomeric states of protein complexes by blue native electrophoresis and isolation of membrane protein complexes by two-dimensional native electrophoresis, Annal. Biochem. 217 (1994) 220–230.
[52] P.O. Ljungdahl, J.D. Pennoyer, D.E. Robertson, B.L. Trumpower, Purification of highly active cytochrome bc1 complexes from phylogenetically diverse species by a single chromatographic procedure, Biochim. Biophys. Acta 891 (1987) 227–241.
[53] H. Schägger, Respiratory chain supercomplexes of mitochondria and bacteria, Biochim. Biophys. Acta 1555 (2002) 154–159.
[54] A. Stroh, O. Anderka, K. Pfeiffer, T. Yagi, M. Finel, B. Ludwig, H. Schägger, Assembly of respiratory complexes I, III and IV into NADH oxidase supercomplex stabilizes complex I in *Paracoccus denitrificans*, J. Biol. Chem. 279 (2004) 5000–5007.
[55] N. Kashani-poor, S. Kerscher, V. Zickermann, U. Brandt, Efficient large scale purification of his-tagged proton translocating NADH:ubiquinone oxidoreductase (complex I) from the strictly aerobic yeast *Yarrowia lipolytica*, Biochim. Biophys. Acta 1504 (2001) 363–370.
[56] I. Marques, N.A. Dencher, A. Videira, F. Krause, Supramolecular organization of the respiratory chain *Neurospora crassa* mitochondria, Eukaryot Cell 12 (2006) 2391–2405.
[57] F. Krause, C.Q. Scheckhuber, A. Werner, S. Rexroth, N.H. Reifschneider, N.A. Dencher, H.D. Osiewacz, OXPHOS supercomplexes, respiration and life-span control in the aging model *Podospora anserina*, Ann. N.Y. Acad. Sci. 1067 (2006) 106–115.
[58] S. De Vries, R. van Witzenburg, L.A. Grivell, C.A.M. Marres, Primary structure and import pathway of the rotenone-insensitive NADH-ubiquinone oxidoreductase of mitochondria from *Saccharomyces cerevisiae*, Eur. J. Biochem. 203 (1992) 587–592.
[59] J.P. Schwitzquébel, J.M. Palmer, Properties of mitochondria as a function of the growth stages of *Neurospora crassa*, J. Bacteriol. 149 (1982) 612–619.
[60] I. Marques, M. Duarte, J. Assunção, A.V. Ushakova, A. Videira, Composition of complex I from *Neurospora crassa* and disruption of two "accessory" subunits, Biochim. Biophys. Acta 1707 (2005) 211–220.
[61] A.L. Umbach, J.T. Wiskich, J.N. Siedow, Regulation of alternative oxidase kinetics by pyruvate and intermolecular disulfide bond redox status in soybean seedling mitochondria, FEBS Lett. 348 (1994) 181–184.
[62] A.H. Millar, M.H.N. Hoefnagel, D.A. Day, J.T. Wiskich, Specificity of the organic acid activation on the alternative oxidase in plant mitochondria, Plant Physiol. 111 (1996) 613–618.
[63] M.N.H. Hoefnagel, A.H. Millar, J.T. Wiskich, D.A. Day, Cytochrome and alternative respiratory pathways compete for electrons in the presence of pyruvate in soybean mitochondria, Arch. Biochem. Biophys. 318 (1995) 394–400.
[64] A.L. Umbach, J.N. Siedow, The cyanide-resistant alternative oxidases from the fungi *Pichia stiptilis* and *Neurospora crassa* are monomeric and lack regulatory features of the plant enzymes, Arch. Biochem. Biophys. 378 (2000) 234–245.
[65] A.G. Medentsev, A.Y. Arinbasarova, N.P. Golovchenko, V.K. Akimenko, Involvement of the alternative oxidase in respiration of *Yarrowia lipolytica* mitochondria is controlled by the activity of the cytochrome pathway, FEMS Yeast Res. 2 (2002) 519–524.
[66] M. Crompton, The mitochondrial permeability transition pore and its role in cell death, Biochem. J. 341 (1999) 233–249.
[67] S. Manon, X. Roucou, M. Guérin, M. Rigoulet, B. Guérin, Characterization of the yeast mitochondrial unselective channel: a counterpart to the mammalian permeability transition pore? J, Bioenerg. Biomembr. 30 (1998) 419–429.
[68] M. Gutiérrez-Aguilar, V. Pérez-Vázquez, O. Bunoust, S. Manon, M. Rigoulet, S. Uribe, In yeast, Ca2+and octylguanidine interact with porin (VDAC) preventing the mitochondrial permeability transition, Biochim. Biophys. Acta 1767 (2007) 1245–1251.
[69] R.A. Zvyagilskaya, M.V. Kovaleva, E.I. Sukhanova, L.A. Ural'skaya, E.S. Guseva, Mitochondria from *Yarrowia lipolytica* yeast do not undergo a typical permeability transition (mPTP), Prooxidants induced only a low-conductance channel for H+. 24th Small Meeting on Yeast Transport and Energetics, 2006, p. 59, 38-A.